UC San Diego
International Symposium on Stratified Flows

Title
Reynolds number effects in stratified turbulent wakes

Permalink
https://escholarship.org/uc/item/1q3025d2

Journal
International Symposium on Stratified Flows, 1(1)

Authors
Diamessis, Peter
Zhou, Qi

Publication Date
2016-08-31

Reynolds number effects in stratified turbulent wakes

Qi Zhou[1] and Peter Diamessis[2]

[1]Department of Applied Mathematics and Theoretical Physics,
University of Cambridge
[2]School of Civil and Environmental Engineering,
Cornell University

Abstract

We report large-eddy simulations of the turbulent wake of a towed-sphere of diameter D at speed U in a linearly stratified Boussinesq fluid with buoyancy frequency N. These simulations are performed using a spectral-multidomain-penalty-method-based incompressible Navier-Stokes solver for $Re \equiv UD/\nu \in \{5 \times 10^3,\ 10^5, 4 \times 10^5\}$ and $Fr \equiv 2U/(ND) \in \{4, 16, 64\}$. Increasingly richer turbulent fine structures are observed in higher-Re wakes within the larger-scale quasi-horizontal vortices at later times, when it is commonly expected that buoyancy has suppressed any turbulent motions. Such phenomenology is examined using the (Re_h, Fr_h^{-1}) phase diagram (Brethouwer et al., 2007). The body-based wake Re is the parameter which determines whether the flow can indeed enter the inviscid strongly stratified regime within which the buoyancy-driven vertical shear layers can either sustain existing turbulence or give rise to secondary shear-instabilities and localized turbulent bursts. The duration of the stratified turbulence regime also scales linearly with Re posing questions on the structural nature of the associated turbulence and its strength with respect to any background motions.

1   Introduction

Stratified turbulent wakes are frequently occurring flows in the stably stratified regions of the ocean and the atmosphere. Of numerous geophysical and naval applications, such flows have motivated extensive research efforts, e.g., as reviewed by Lin and Pao (1979) and Spedding (2014). In this paper, we focus on stably stratified towed-sphere wakes, a canonical flow involving both shear and buoyancy forces, which are described by Reynolds number $Re \equiv UD/\nu$ and Froude number $Fr \equiv 2U/(ND)$, where D is the sphere diameter, U is the tow speed, N is the buoyancy frequency, and ν is the kinematic viscosity.

The numerical dataset presented in this paper is generated through large-eddy simulations using a spectral-multidomain-penalty-method-based incompressible Navier-Stokes solver (Diamessis et al., 2005). This solver employs Fourier discretization in both horizontal directions x (streamwise) and y (spanwise), and a Legendre-polynomial-based spectral multidomain scheme in the vertical direction z. Spectral filtering and a penalty scheme ensure the numerical stability of the simulations without resolving the full spectrum of turbulent motions. Details on the configuration of these stratified wake simulations can be found in Diamessis et al. (2011) (hereinafter referred to as 'DSD').

In this paper, we present preliminary results on the influence of Re on wake turbulence by examining the numerical dataset produced by Zhou (2015) at $Re \in \{5 \times 10^3,\ 10^5, 4 \times 10^5\}$ and $Fr \in \{4, 16, 64\}$. Prior simulations by DSD up to $Re = 10^5$ demonstrate the prolongation of the duration of the non-equilibrium regime (Spedding, 1997) with increasing Re value due to localized secondary shear instabilities within the wake, consistent with the 'stratified turbulence' hypothesis by Lilly (1983) and the pioneering computational study

by Riley and de Bruyn Kops (2003). The effects of varying Re in wakes have also been seen in terms of the internal waves emitted by the wake turbulence (Abdilghanie and Diamessis, 2013; Zhou and Diamessis, 2016) and the properties of the turbulent/non-turbulent interface (Watanabe et al., 2016). The dataset recently produced by Zhou (2015) brings into play an additional Re data point at $Re = 4 \times 10^5$. As such it enables an unprecedented systematic investigation of Re effects on the wake turbulence. Hereinafter, each simulation will be labelled as RaFb, where $a = Re/10^3$ and $b = Fr$.

Significant progress in stratified turbulence theory has recently been made, as reviewed by Riley and Lindborg (2012). Scaling arguments (Riley et al., 1981; Lilly, 1983; Billant and Chomaz, 2001; Brethouwer et al., 2007) based on the Navier-Stokes equations lead to the prediction of a distinct 'strongly stratified turbulence' regime where stratification is strong and viscous effects are weak. An instructive way to identify the potential presence of such a regime in any given flow is through a diagram plotted on the (Re_h, Fr_h^{-1}) phase space, where Re_h and Fr_h are appropriately defined Reynolds and Froude numbers based on horizontal turbulent motions. Within the strongly stratified regime where $Re_h \gg 1$ and $Fr_h \ll 1$, the formation of buoyancy-driven layers of concentrated shear takes place independently of viscosity with the layer thickness scaling as $\mathcal{U}/N$, where $\mathcal{U}$ is a turbulent horizontal velocity scale. Existing studies on this regime mainly focus on homogeneous flows (e.g., Riley and de Bruyn Kops (2003); Brethouwer et al. (2007)). The primary aim of this paper is to investigate in the stratified turbulent towed-sphere wake, a canonical localized inhomogeneous turbulent flow, in the context of stratified turbulence theory. The particular focus lies on characterizing the dependence of coherent vortical structures on Re, the scaling of various turbulent diagnostics with Re, the associated persistence time of stratified turbulence within the wake and the associated trajectories in (Re_h, Fr_h^{-1}) phase space.
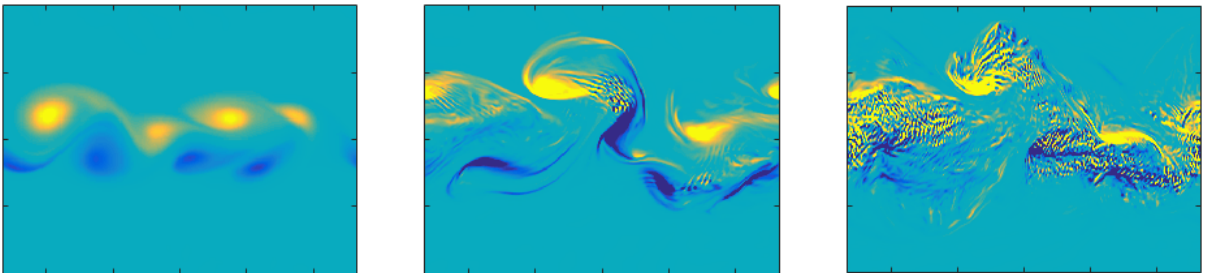
2 Flow structure

Figure 1: Contour plots of vertical vorticity ω_z at $Nt = 150$ sampled at the Oxy horizontal mid-plane for simulations at $Re \in \{5 \times 10^3, 10^5, 4 \times 10^5\}$ respectively (from left to right) and $Fr = 4$. Sphere travels from left to right. The size of the visualization window is $\frac{80}{3}D$ in x and $20D$ in y.

Figures 1 and 2 show contour plots of the vertical, ω_z, and spanwise, ω_y vorticity on the Oxy and Oxz wake centerplanes in the wake flow in both horizontal and vertical directions at a later time of $Nt = 150$. The ω_y snapshots are supplemented with an earlier time at $Nt = 50$. More details on the evolution of the wake structure may be found in §7.2 of Zhou (2015). At both of these times, the R5F4 run has progressed well into the quasi-two-dimensional (Q2D) regime, where quasi-horizontal 'pancake' vortices
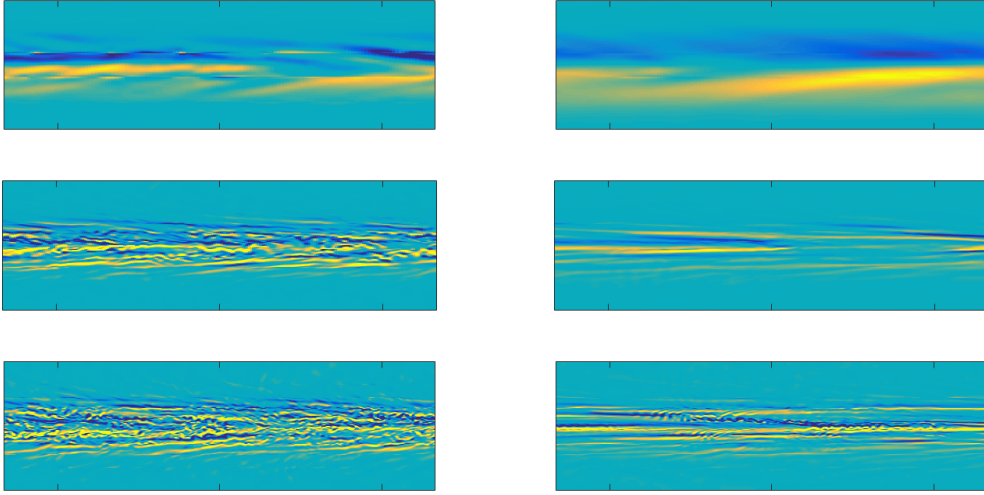
Figure 2: Contour plots of spanwise vorticity ω_y at $Nt = 50$ (left panel) and 150 (right panel) sampled at the Oxz vertical mid-plane for simulations at $Re \in \{5 \times 10^3, 10^5, 4 \times 10^5\}$ respectively (from top to bottom) and $Fr = 4$. Sphere travels from left to right. The size of the visualization window is $\frac{40}{3}D$ in x and $4D$ in z.

dominate the flow and grow through vortex pairing and vortex diffusion (Spedding, 2002). Vertical transects of ω_y show, at both times, strongly inclined shear layers which diffuse even further over time and remain stable to any perturbations. In contrast, for the two higher Re runs, the thickness of these layers is markedly reduced. Kelvin-Helmholtz instabilities, resulting in localized secondary patches weak of turbulence as reported by Riley and de Bruyn Kops (2003) and DSD, are visible. These secondary events are far more space-filling for the R400F4 case, persisting as late as $Nt = 150$. The equivalent signature of these events on the Oxy centerplane is evident in figure 1 where significant fine structure is embedded within large-scale quasi-horizontal motions in R400F4. In contrast, at R100F4, only a couple patches of turbulent motion remain at these later times. Overall, these observations suggest that 'stratified turbulence' is operative at the two higher Re shown here: an inverse cascade occurs in the horizontal, driven by pancake vortex pairing, competing against a forward cascade associated with shear-driven turbulence.

3 Stratified turbulence statistics

3.1 Turbulence Decay

The evolution of the buoyancy Reynolds number Re_b is shown in figure 3. Although, formally, one defines $Re_b \equiv \varepsilon/(\nu N^2)$, where ε is the turbulence kinetic energy dissipation rate, in this case the buoyancy Reynolds number is approximated through $Re_b \approx Re_h Fr_h^2$, an approximation valid at least for $Re_b > O(1)$ (Hebert and de Bruyn Kops, 2006). Here the horizontal local/turbulent Reynolds and Froude numbers are defined as $Re_h = \mathcal{U}\ell_h/\nu$ and $Fr_h = \mathcal{U}/(N\ell_h)$, where $\mathcal{U}$ is taken as the volume-averaged root-mean-square horizontal velocity on the horizontal planes with the largest vertical shear (DSD) and ℓ_h is the horizontal integral scale following equation (5.5) of DSD. Re_b is a measure of the dynamic range in stratified turbulence, i.e. the scale separation between Ozmidov and Kolmogorov

scale (Hebert and de Bruyn Kops, 2006). Effectively, when Re_b is sufficiently greater than unity, a significant range of turbulent scales of motion can operate in a strongly stratified environment with $Fr_h \ll 1$. The left panel of figure 3 indicates that this unity-crossing time is delayed with increasing Re, with $Re_b \approx 1$ occurring at $Nt \approx 10$, 150 and 400 for $Re = 5 \times 10^3$, 10^5 and 4×10^5. This observation suggests an increasingly broader and persistent spectrum of turbulent motions within a stratified wake following the onset of buoyancy control at $Nt \approx 2$. Rescaling the vertical axis with $1/Re$ leads to a rough collapse of all curves (figure 3, right panel) which indicates that, indeed, the unity crossing time of Re_b does scale linearly with Re.

Further probing the persistence of stratified turbulence, as evidenced by values of $Re_b \gg 1$ during stratified wake evolution, figure 4 shows the time history of all three root-mean-square fluctuating velocities in the F4 simulations. At lower Re, $w' \ll u'$ and v'. Driven by later-time stratified turbulence, the magnitude of w' increases with Re remaining as large as 20% of u' and 1% of the reference tow speed U up to time $Nt \approx 150$. .
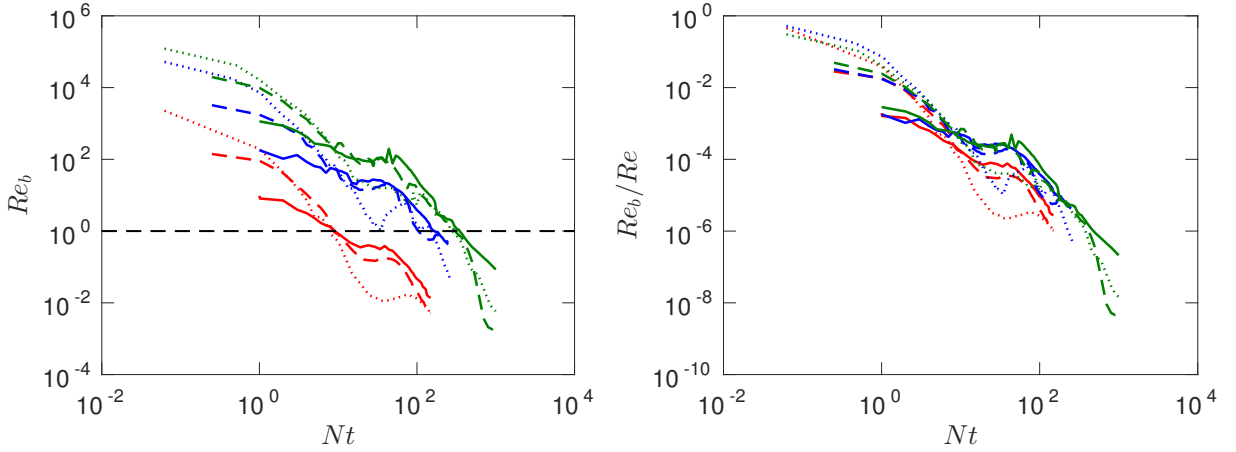

Figure 3: Left panel: the buoyancy Reynolds number Re_b, approximated by $Re_h Fr_h^2$, as a function of Nt. Right panel: Re_b rescaled by the wake Reynolds number Re. $Re = 5 \times 10^3$ in red, $Re = 10^5$ in blue, and $Re = 4 \times 10^5$ in green; $Fr = 4$, 16 and 64 are in solid, dashed and dotted lines respectively.

3.2   Turbulent length scales

The time history of horizontal integral scale ℓ_h and the volume-averaged vertical Taylor scale ℓ_v (defined in Riley and de Bruyn Kops (2003)) is shown in figure 5. The evolution of ℓ_h does not seem to be strongly dependent on the wake parameters Re and Fr. ℓ_v for the R100 and R400 runs follows the inviscid $\mathcal{U}/N$ scaling proposed by Billant and Chomaz (2001), indicating that the buoyancy-generated vertical shear layers are not subject to viscous diffusion and are highly prone to shear instability as shown in figure 2. Note that the starting time of the window during which the R100 (blue) and R400 (green) lines collapse, i.e., $Nt \approx 10$, corresponds to the time when Fr_h (see figure 7.14 of Zhou (2015)) drops below $O(0.1)$ while Re_h remains sufficiently large, providing further support that the wake has entered the near-inviscid stratified turbulence flow regime. The R5 data (red) do not follow the same scaling, as Re_h is significantly smaller at times $Nt \geq 10$ and $Re_b \ll 1$. Instead, as suggested by Brethouwer et al. (2007), the low Re data follow the viscous scaling $\ell_v/\ell_h \sim Re_h^{-1/2}$ (see figure 7.18 of Zhou (2015)).
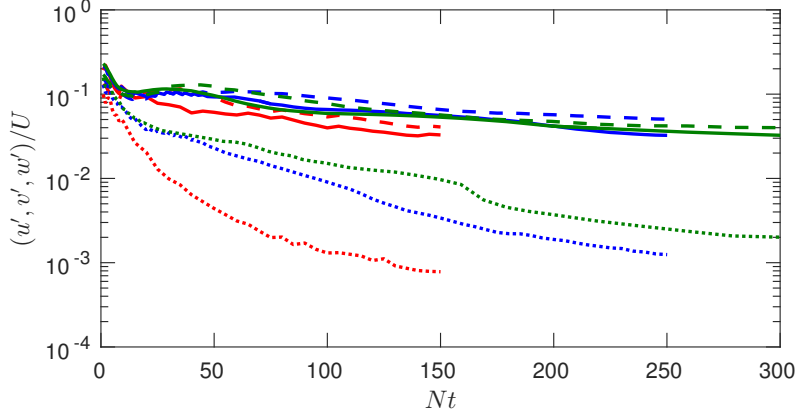
Figure 4: Time evolution of root-mean-square velocity fluctuations (u', v', w') which are normalized by tow speed U for simulations at $Fr = 4$. The velocity scales are volume-averaged over $-L_y < y < L_y$ and $-L_z < z < L_z$, where L_y and L_z are the half width/height of the mean wake. $Re = 5 \times 10^3$ in red, $Re = 10^5$ in blue, and $Re = 4 \times 10^5$ in green; u', v' and w' are in solid, dashed and dotted lines respectively.
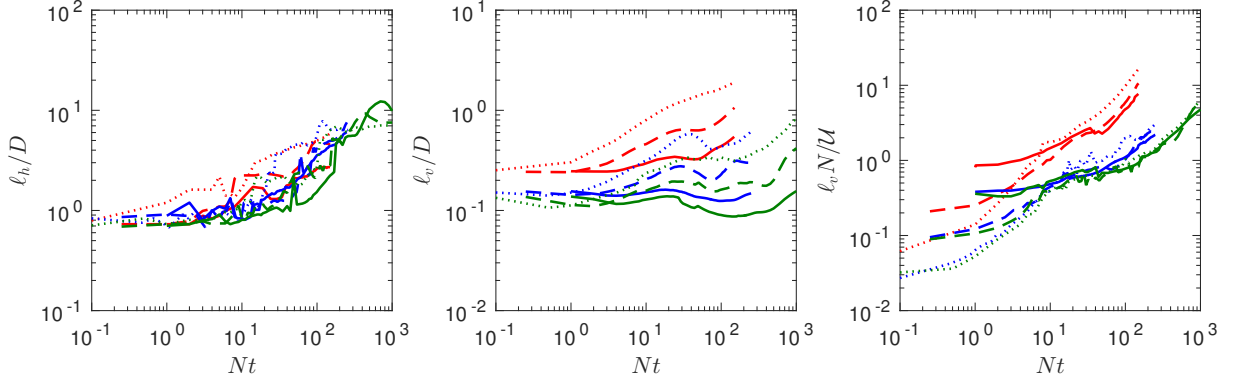

Figure 5: Time evolution of horizontal and vertical Taylor scales ℓ_h and ℓ_v, both normalized by sphere diameter D, plotted in Nt unit. The right most panel shows ℓ_v rescaled with the inviscid strongly stratified scaling $\ell_v \sim \mathcal{U}/N$ (Billant and Chomaz, 2001). Line legends are the same as figure 3.

3.3 Evolution in the phase space

Finally, it is instructive to examine the trajectory of a wake across different stratified flow regimes in (Re_h, Fr_h^{-1}) phase space (Brethouwer et al., 2007). For a fixed value of $Fr = 4$ (figure 6, left panel), the wake initially operates in the weakly stratified regime with initially large ε and $\mathcal{U}$ and, hence, large Re_b and Fr_h. The fact that the trajectory's starting point, at least for the $Fr = 4$ data does not reside in the classical Kolmogorov turbulence regime, associated with active turbulence uninhibited by buoyancy, may be an artifact of the approximations involved in designing the initial condition while not explicitly accounting for the sphere. The interested reader is referred to DSD and Zhou and Diamessis (2016) for additional discussion. Note that the initial Re_b, measured graphically by the distance of the wake trajectory to its projection onto the diagonal line indicating $Re_b \approx Re_h Fr_h^2 = 1$, is set by the wake's Re. As the wake evolves, on one hand, Re_h stays relatively constant. This is because the increase in ℓ_h compensates for the decrease of $\mathcal{U}$ (Hebert and de Bruyn Kops, 2006). On the other hand, the increase of ℓ_h and decrease of
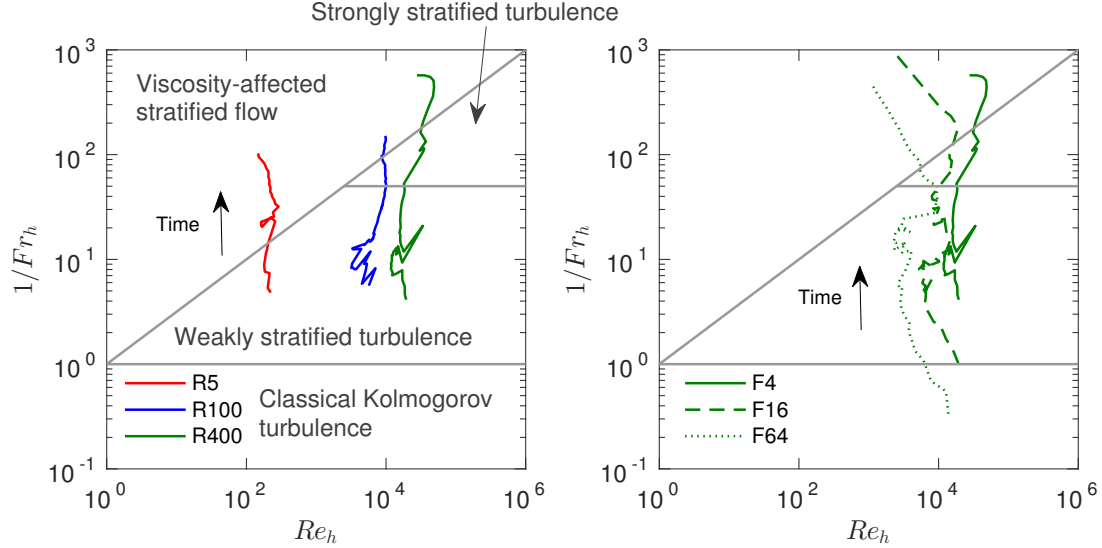
Figure 6: Evolution of wake turbulence in the (Re_h, Fr_h^{-1}) phase space at $Fr = 4$ for all three Re values (left panel) and at $Re = 4 \times 10^5$ for all three Fr values (right panel). The classification of the flow regimes is after figure 18 of Brethouwer et al. (2007).

$\mathcal{U}$ result in the decrease of Fr_h. Re is effectively the factor which determines whether the flow enters the viscously dominated regime and bypasses the strongly stratified turbulence regime, characterized by $Re_h \gg 1$, $Fr_h \ll 1$ and secondary turbulence events, before the wake becomes viscously dominated. The higher the value of Re, the higher Re_b (or Re_h) becomes, and the longer the time the wake spends in the strongly stratified regime, as evidenced by comparing the trajectories of R100F4 and R400F4. R5F4 does not enter the strongly stratified regime as small $Fr_h \ll 1$ never coexists with sufficiently large Re_b in wake evolution.

Fixing $Re = 4 \times 10^5$, one may focus on the Fr dependence of phase space trajectories (figure 6, right panel). The trajectory shifts to smaller values of Re_h with increasing Fr (see figure 7.14 of Zhou (2015)). This is expected because, while ℓ_h/D is weakly Fr-dependent (see figure 5), the velocity scale $\mathcal{U}$ scales with the mean centerline defect velocity U_0 in a Fr-dependent manner (Spedding, 1997; Diamessis et al., 2011; Zhou, 2015). The higher the wake Fr value, the lower the value of $\mathcal{U}$ upon onset of buoyancy control, which is not compensated by the corresponding increase in ℓ_h/D with Fr at this time, and the lower the value of Re_h. The question that then emerges, similar to the inquiry explored by Spedding (1997), is whether, for a given Re and sufficiently large Re_b, there exists a critical Fr above which the flow cannot traverse the strongly stratified regime.

4   Discussion

The availability of three sphere-based Re values of 5×10^3, 10^5 and 4×10^5 has enabled a first preliminary effort into quantifying the Reynolds number dependence of stratified turbulent wakes which gives rise to several intriguing questions. The linear Re scaling of the unity-crossing time of Re_b, as approximated by $Re_b \approx Re_h Fr_h^2$, poses questions about the persistence of a stratified wake at values typical of ocean engineering applications and geophysical flows. On one hand, $Re_h Fr_h^2 = 1$ and not $Fr_h = 1$, which has been

proposed by lower Re-focused investigations, should be the most appropriate condition for setting turbulent vertical momentum transport to zero in a wake in predictive self-similarity models (Meunier et al., 2006). On the other hand, one wonders about the duration of the initial fraction of the $Re_h Fr_h^2 > 1$ interval during which the stratified turbulence is distinguishable with respect to any background motions. To this end, how strong does the root-mean-square w' have to be with respect to the tow speed U and possibly the wake centerline velocity U_0? In addition, how does the nature of stratified turbulence change as the fraction of the wake trajectory in the stratified turbulence regime of the (Re_h, Fr_h^{-1}) phase space becomes larger with increasing Re? Are the secondary Kelvin-Helmholtz instabilities and resultant turbulence less intermittent during the initial stages of this regime, corresponding to a highly anisotropic and layered form of space-filling turbulence? Further analysis of the existing wake data and stratified homogeneous turbulence datasets (de Bruyn Kops, 2015) will help answer the above questions as will also additional simulations at even higher Re, possible only when greater computing power is available.

Acknowledgement

References

Abdilghanie, A. M. and Diamessis, P. J. (2013). The internal gravity wave field emitted by a stably stratified turbulent wake. *J. Fluid Mech.*, 720:104–139.

Billant, P. and Chomaz, J.-M. (2001). Self-similarity of strongly stratified inviscid flows. *Phys. Fluids*, 13:1645.

Brethouwer, G., Billant, P., Lindborg, E., and Chomaz, J.-M. (2007). Scaling analysis and simulation of strongly stratified turbulent flows. *J. Fluid Mech.*, 585:343–368.

de Bruyn Kops, S. M. (2015). Classical scaling and intermittency in strongly stratified Boussinesq turbulence. *J. Fluid Mech.*, 775:436–463.

Diamessis, P. J., Domaradzki, J. A., and Hesthaven, J. S. (2005). A spectral multidomain penalty method model for the simulation of high Reynolds number localized incompressible stratified turbulence. *J. Comput. Phys.*, 202:298–322.

Diamessis, P. J., Spedding, G. R., and Domaradzki, J. A. (2011). Similarity scaling and vorticity structure in high-Reynolds-number stably stratified turbulent wakes. *J. Fluid Mech.*, 671:52–95, referred to in the text as 'DSD'.

Hebert, D. A. and de Bruyn Kops, S. M. (2006). Predicting turbulence in flows with strong stable stratification. *Phys. Fluids*, 18:066602.

Lilly, D. K. (1983). Stratified turbulence and the mesoscale variability of the atmosphere. *J. Atoms. Sci.*, 40:749–761.

Lin, J.-T. and Pao, Y.-H. (1979). Wakes in stratified fluids. *Ann. Rev. Fluid Mech.*, 11:317–338.

Meunier, P., Diamessis, P. J., and Spedding, G. R. (2006). Self-preservation in stratified momentum wakes. *Phys. Fluids*, 18:106601.

Riley, J. J. and de Bruyn Kops, S. M. (2003). Dynamics of turbulence strongly influenced by buoyancy. *Phys. Fluids*, 15:2047.

Riley, J. J. and Lindborg, E. (2012). Recent progress in stratified turbulence. In Davidson, P. A., Kaneda, Y., and Sreenivasan, K. R., editors, *Ten Chapters in Turbulence*, pages 269–317. Cambridge University Press.

Riley, J. J., Metcalfe, R. W., and Weissman, M. A. (1981). Direct numerical simulations of homogeneous turbulence in density-stratified fluids. *AIP Conf. Proc.*, 76:79–112.

Spedding, G. R. (1997). The evolution of initially turbulent bluff-body wakes at high internal Froude number. *J. Fluid Mech.*, 337:283–301.

Spedding, G. R. (2002). Vertical structure in stratified wakes with high initial Froude number. *J. Fluid Mech.*, 454:71–112.

Spedding, G. R. (2014). Wake signature detection. *Ann. Rev. Fluid Mech.*, 46:273–302.

Watanabe, T., Riley, J. J., de Bruyn Kops, S. M., Diamessis, P. J., and Zhou, Q. (2016). Turbulent/non-turbulent interfaces in wakes in stably stratified fluids. *J. Fluid Mech.*, 797:R1.

Zhou, Q. (2015). *Reynolds number scaling of a localized stratified turbulent flow and far-field evolution of turbulence-emitted internal waves.* PhD thesis, Cornell University, Ithaca, New York.

Zhou, Q. and Diamessis, P. J. (2016). Surface manifestation of internal waves emitted by submerged localized stratified turbulence. *J. Fluid Mech.*, 798:505–539.